U.S. ENVIRONMENTAL PROTECTION AGENCY
REGION IX
SAN FRANCISCO, CA

Explanation of Significant Differences
To the October 30, 2023 Record of Decision
For the Iron King Mine – Humboldt Smelter Superfund Site
January 2025

I.   Purpose of Document

The U.S. Environmental Protection Agency (EPA) is issuing this Explanation of Significant Differences (ESD) to establish and explain differences in the remedial requirements for the response action selected by the Record of Decision (ROD) issued by EPA on October 30, 2023 for the Iron King Mine – Humboldt Smelter Superfund Site (Site). (EPA Doc I.D. # R9-10034911). EPA is the lead agency for the Site, and the Arizona Department of Environmental Quality (ADEQ) is the support agency. Section 117(c) of CERCLA and Section 300.435(c)(2)(i) of the NCP require publication of an ESD when it is determined by EPA that changes to the original selected remedy are significant, but do not fundamentally alter the remedy selected in the ROD with respect to scope, performance, or cost. This ESD provides the public with an explanation of the modification to the selected remedy, summarizes the information that supports this modification, and confirms that the revised remedial action complies with the statutory requirement of Section 121 of CERCLA, 42 U.S.C. § 9621.

II.   Site History and Contamination

The Site is in the town of Dewey-Humboldt (pop. 4,455) in Yavapai County, Arizona. It is situated on Arizona State Highway 69 about 80 miles north of Phoenix, Arizona, and 80 miles south of Flagstaff, Arizona. There is a legacy of mining and smelting in this area.

The Site encompasses locations with contamination from two historical industrial operations: the former Iron King Mine and the former Humboldt Smelter. Zinc, lead, silver, and gold ores were mined and concentrated at the Iron King Mine between about 1910 and 1968. The former mine property contains a mine tailings pile of 4 million cubic yards that is high in arsenic and lead. The Humboldt Smelter and two older facilities at generally the same location operated from the late 1800s until about 1937, crushing copper and lead ores and melting them in furnaces to make pure metal. Wind carried away particulates from the smelter smokestacks. Mine tailings, a waste called dross (a fine-grained, gray-colored waste that forms on top of certain kinds of molten metals), slag (a lava-like earthen waste left over after the metal of interest is removed by smelting), and soils contaminated with lead and other metals remain on the smelter property. Both the former mine and smelter properties are located on the Chaparral Gulch, a major drainage that passes into Dewey-Humboldt from the west. The Chaparral Gulch drains from tributaries in the mountains west of the Site and empties into the Agua Fria River on the east side of the Site.

Historical operations at the facilities left behind millions of tons of mine and smelter wastes, including extensive mine tailings, mixed alluvium and tailings, waste dross, smelter slag and contaminated soils. These wastes have migrated to the Chaparral Gulch, other surface water drainages at and near the former mine and smelter properties, and some soils in residential areas of Dewey-Humboldt. Shallow groundwater is affected, but only directly below the primary wastes.

Starting in 2002, EPA and ADEQ conducted preliminary investigations at the Site. EPA proposed the Site for listing on the Superfund program's National Priorities List (NPL) in March 2008 and formally listed the Site on the NPL in September 2008. EPA, ADEQ and other parties have performed numerous removal actions at the Site, beginning in 2006 and completing in 2022. Three of these actions (2006, 2011 and 2017) consisted of cleanup of residential soil contamination. Contaminated soils at 47 properties were excavated to a maximum depth of 2 feet and replaced with clean soil. The Remedial Investigation (RI) was completed in 2016. The Feasibility Study (FS) was completed in 2022.   There is presently one operable unit for the Site.

III.   Selected Remedy

As with many mine and smelter sites, this Site poses a number of complex problems and technical challenges in dealing with large volumes of waste (tailings, mixed tailings and alluvium, dross, slag and waste rock) and other contamination found in many different environments and locations. In the ROD, the Site was broken down into three areas:

1) Non-residential or "waste" areas, including the mine and smelter properties and the contaminated drainages between them, where the mine/smelter wastes are located;

2) Residential properties with site-related contamination; and

3) Shallow groundwater beneath the waste areas.

The significant differences discussed in this document pertain to selected response actions for properties with residential anticipated future land use. The remedy selected by the ROD required the excavation of contaminated residential surface soils where exposure point concentrations of Site chemicals of concern (COCs) exceeded cleanup levels for 6 metals established in the ROD: arsenic, lead, cobalt, antimony, manganese, and thallium. The ROD required the replacement of the contaminated soils with clean soil, and restoration of the properties. The cleanup levels in the ROD for each COC are shown in *Table 1*, expressed in milligrams per kilogram (mg/kg).

Table 1. Residential Surface Soil Cleanup Levels for COCs

Arsenic*	Lead	Cobalt	Antimony	Manganese	Thallium
48 west of river 78 east of river	200	44	31	1800	2.8

Values shown are expressed in milligrams per kilogram (mg/kg)

*Cleanup levels for arsenic were based on background levels that vary due to geology depending on location of properties relative to the Agua Fria River. This results in 2 location-specific cleanup levels for arsenic.

In the non-residential, "waste areas," the ROD specified excavation and consolidation of wastes and contaminated soils into two permanently capped waste repositories. The ROD selected an

interim remedy for groundwater to limit groundwater use until a final groundwater remedy can be selected. The significant differences discussed in this document pertain to the response actions selected for the areas with residential anticipated future land use and are not related to the non-residential / waste areas or groundwater that are also addressed in the ROD.

IV.   Basis for Changes from the Record of Decision

Background/Context

In several sampling events conducted during the RI which was completed in 2016, EPA collected thousands of samples from over 500 residential properties. Data from the RI supported the 2017 removal action and the ROD. After the ROD was issued in 2023, the following factors contributed to the need for additional sampling at residential properties during the remedial design phase:

- The ROD selected lower cleanup levels for arsenic and lead than had been used in previous actions;

- The background concentrations for arsenic were lowered and due to geological variability in background concentrations, split into two values, one for areas east and another for areas west of the Agua Fria River; and

- To ensure a comprehensive evaluation and cleanup every property was divided into quarter-acre exposure units (EUs) and sampled at a fixed sample density.

Application of these three factors results in additional properties that will require cleanup. Accordingly, as of the date of this ESD, approximately more than 7200 additional soil samples have been collected at more than 200 residential properties to determine which properties are to be identified for cleanup in accordance with the ROD.

Manganese

The ROD set a residential cleanup level of 1800 mg/kg for manganese (*See Table 1 above and ROD Tables 6 and 7)*. The cleanup level was based on a noncancer hazard index of 1 under the child-only scenario. The corresponding value for the adult-only scenario is 16,000 mg/kg. Manganese has a *regional* background threshold value (expressed as the 95%-95% Upper Tolerance Level) of about 1600 mg/kg. Regional background values for metals in soils at the Site were determined based on more than 500 measurements in soils beyond the Area of Potential Site Impact (RI Report, Appendix E).
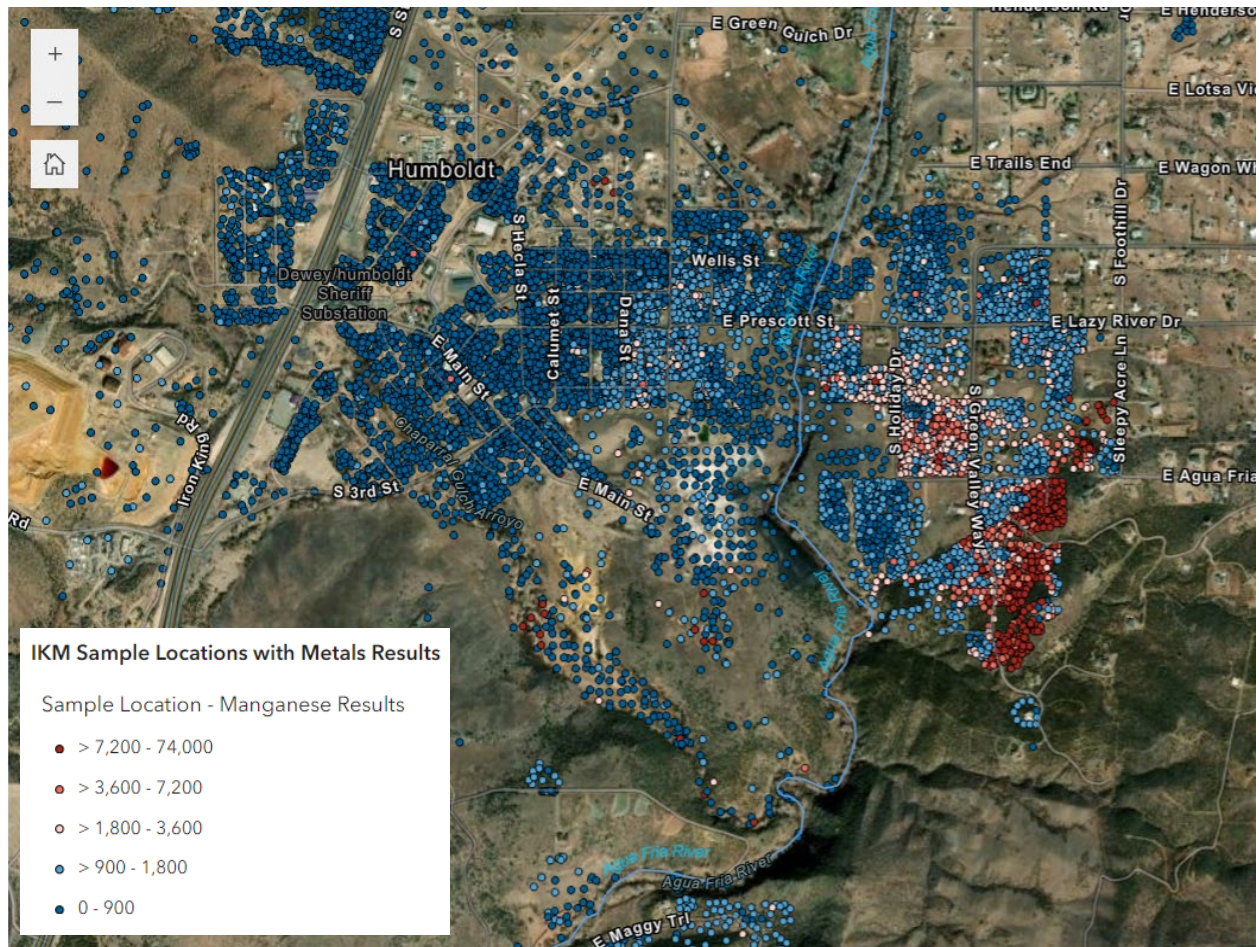
Figure 1: Manganese concentrations in surface soils. Sample points plotted in blue are below the ROD cleanup standard for manganese. Sample points plotted in red are above the cleanup level. See legend for concentration ranges. The Agua Fria River is depicted by the blue wobbly line.

Elevated Levels of Manganese at Localized Residential Properties

During the current 2024 sampling effort, uncharacteristically high levels of manganese have been discovered over a localized area of residential properties, the distribution of which is very heavily weighted spatially on the east side of the Agua Fria River. This area is of a more limited and smaller scale than regional background. The individual sample concentrations are as high as approximately 47,000 mg/kg (4.7%). Of the 6962 recent sample results for manganese (and 2194 sample results from previous years), 1317 manganese results exceed the cleanup level of 1800 mg/kg. The average concentration is about 2400 mg/kg. Concentrations of manganese exceed 10,000 mg/kg in 184 samples. In the most recent sampling effort, the exposure point concentration (EPC) (95% upper confidence level on the mean) of manganese exceeds the

cleanup level at about 195 out of 823 exposure units[1] (1/4-acre properties or portions of properties) for which initial data are available for this analysis.

The distribution of manganese concentrations can be seen in *Figure 1*. Samples shown in light or dark red are above the residential cleanup level specified in the ROD; samples shown in light or dark blue are below the below the residential cleanup level specified in the ROD. The concentrations corresponding to colors can be seen in the legend on the figure. For concentrations above the residential cleanup level specified in the ROD, the color pink corresponds to concentrations between 1800 mg/kg (cleanup level) and 3600 mg/kg (twice the cleanup level); the color red corresponds to concentrations between 3600 mg/kg and 7200 mg/kg; the color dark red corresponds to concentrations above 7200 mg/kg up to the maximum level of 47,000 mg/kg.

Sampling has demonstrated that concentrations of manganese increase from west to east across the Site. The underlying geology changes at the Agua Fria River.

Manganese concentrations are considerably higher in localized areas east of the river and highest on the slopes of a mountain ridge (facing away from the smelter) on the east side of the river. Concentrations of manganese in residential soil near the former mine tailings pile are well below the cleanup level. Residential surface soil near the former smelter (including immediately across the river from the smelter), has low manganese concentrations, but the manganese concentrations become higher in localized areas to the east, and then still farther east, the manganese concentrations become lower, similar to regional background levels.

Determining the Source of Elevated Manganese

While the regional background of manganese is below the residential cleanup level specified in the ROD, the discovery of the elevated levels of manganese shown above required a determination of the source of the manganese and whether the elevated manganese is either naturally occurring or site related. EPA considered whether the manganese levels were the result of a localized surface geological expression that has influenced the soil development, indicating it is naturally occurring. This would be independent of the regional background levels of manganese. Alternately, if the manganese were site related, there would be three potential transport pathways for the manganese in residential soils:

---

[1] An exposure unit is a quarter-acre area within a property where a receptor could reasonably spend their time over many years while exposed to soil. Small properties may have only one exposure unit. Larger properties may have several exposure units in case the property is later divided up into subparcels. Residential properties at the Site vary from about 0.1 acre to 8 acres and the use of exposure units of uniform size ensures that exposure point concentrations correspond to accurate risks. Cleanup may be necessary on one exposure unit but not others within the same property.

- Blowing tailings from the mine or the smelter[2];

- Blowing dross wastes from the smelter; or

- Fallout of particulate matter from historical stack emissions at the smelter (prior to 1937).

To address this matter, EPA has examined various evidence and performed two separate studies which are described below. Based on this analysis, EPA has determined that the localized elevated manganese levels in residential soils are naturally occurring and are *not* site related. This phenomenon is due to localized geology that results in higher manganese soil concentrations than the regional background based on the following evidence:

1. **The levels of manganese in mine tailings and dross at the Site are far too low to account for the high localized manganese concentrations found in residential soil** (up to 47,000 mg/kg). This rules out the possibility that the source of high soil manganese is blowing tailings or dross. Tables 2 and 3 below show the levels of manganese in waste dross at the smelter, and in the tailings at the mine tailings pile. Manganese levels were *below* the cleanup levels in all 160 tailings samples at the former mine and in over 99% of the 559 samples of the dross at the former pyrometallurgical operations area at the smelter. Moreover, the maximum concentration of manganese in the five (0.9% of samples) samples of the dross above the cleanup level was 2,830 mg/kg, more than 16 times less than the maximum concentration above 47,000 mg/kg observed in residential samples.

Table 2

Manganese in Pyrometallurgical Operations Area (NR11) with Smelter Waste Dross	
Number of Samples	559
Number of Dross Samples with Manganese at Levels above Residential Cleanup Level of 1800 mg/kg	5 (0.9%)
Maximum Concentration	2830
Average Concentration	747 mg/kg
95% UCL of Concentration	771 mg/kg

---

[2] The mine operated from the first decade of the 20th century until 1968. The main Humboldt smelter operated from about 1906 to 1937. While smelting operations themselves do not produce mine tailings, there was also some ore concentrating done at the smelter property, both by the owners of the Humboldt Smelter and by an operator who attempted to concentrate ores after the smelter stopped operations.

Table 3

Manganese in the Tailings at the Iron King Mine Main Tailings Pile	
Number of Samples (XRF and Laboratory)	160
Number of Tailings Samples with Manganese at Levels above Residential Cleanup Level of 1800 mg/kg	0
Maximum Concentration	1710 mg/kg
Average Concentration	934 mg/kg

2. **Manganese is not a volatile metal; its vapor pressure is so low that it is not expected to have been contained and transported in stack emissions from the smelter at any significant concentration (much less up to 4.7% exhibited in residential samples).[3] The probability of such concentrations being attributable to fallout of particulates from manganese emissions from the smelter after mixture and dilution into soils is diminishingly small.** The volatility of manganese at the temperatures of copper smelting (1500 °C) is low and similar to that of iron at the same temperature. Given the applicable equations (shown in *Attachment A*), the vapor pressure of manganese in stack emissions would be about 34 pascal (Pa) at the maximum expected copper smelting temperature. This is about 3 ten thousandths of one atmosphere, which is negligible and would result in virtually no stack emissions of manganese.

3. **The U.S. Geologic Survey bedrock geology (**https://pubs.usgs.gov/sim/2996/downloads/pdf/2996_map.pdf**) indicates that the area of highest manganese concentrations in soils directly coincides with a localized outcrop of siliceous iron formation that would be expected to contain higher levels of manganese.** This supports a conclusion that the manganese levels are the result of a localized surface geological expression of underlying bedrock that has influenced soil development. Soils formed from rock weathering subsequently spread downhill by erosion over time. *Figure 1* shows the areas of elevated manganese data. *Figure 2* shows a portion of the USGS map with the bedrock labeled "Xi" and the description of "Iron formation, metachert, and siliceous metamorphic rocks" which is a member of the Spud Mountain Volcanics. The metacherts indicate a sedimentary origin of the rock. *Figure 2* also shows the area of elevated manganese overlaid on the geologic map. As shown, the manganese closely matches the mapped location of the iron formation (Xi). The formation is localized. Iron and manganese are well understood to co-occur in sedimentary iron formations due to their similar properties and location on the periodic table (see for example Lepp, H., *The*

---

[3] A volatile metal more readily turns to vapor upon heating (as in smelting). Examples of volatile metals include zinc and arsenic.

Relation of Iron and Manganese in Sedimentary Iron Formations, Economic Geology (1963) 58(4) 515-526). The statistical multivariate compositional analysis discussed below also shows a high correlation between iron and manganese. This evidence indicates that the area of elevated manganese in residential soils is the result of the underlying mineralogy and is naturally occurring.
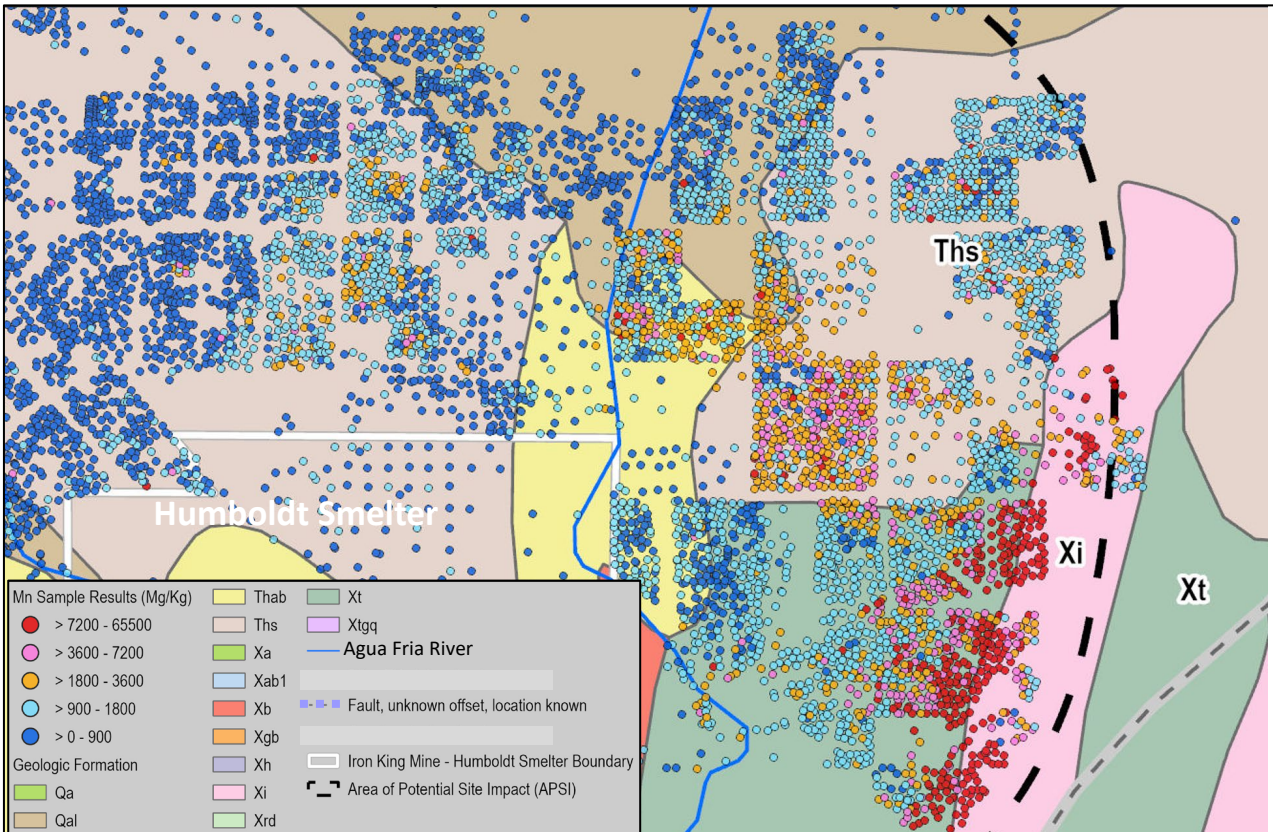

Figure 2. Local geology near Humboldt Smelter overlaid by manganese concentration plot

4. **EPA performed a statistical multivariate compositional cluster analysis indicating that the relative composition of manganese and five other metals in the soils is consistent with a natural source and inconsistent with a site-related source.** This type of analysis examines the geospatial and constituent ratio distribution (six-dimensional concentration ratios) to evaluate the nature of the source of a material in a localized area. The report is attached to this ESD as *Attachment A*. The compositional and spatial aspects of the sampling data for six metals indicate that the areas with substantially elevated manganese concentrations, especially east of the Agua Fria River, are part of a mid-scale spatial pattern that indicate they are naturally occurring. These areas have similar metals compositional aspects to the vast majority of the study area but have elevated manganese due to higher iron concentrations. Geochemical association of several elements with iron, especially manganese and arsenic, is common and occurs naturally. This phenomenon is widespread across the Site and likely associated with soil minerals. There is variation in iron

concentrations across the site. In areas where iron concentrations are higher, manganese concentrations also tend to be higher.

5. **Based on new sampling data collected in the summer of 2024, EPA performed another statistical study that evaluated manganese concentration trends with soil depth. The study indicates that the high manganese levels in residential soils are not site related**. It would be expected that fallout of particulate matter from stack emissions would settle into soils at or near the surface. It would therefore result in statistically higher manganese concentrations at shallow depth (e.g. 2-4 inches), as compared to concentrations at greater depths (e.g. 6 to 12 inches) which would be lower and more consistent with regional background concentrations. However, this trend was not observed in EPA's recent soil sampling. Levels of manganese with depth were more-or-less uniform, indicating that the manganese is derived from localized geology during soil formation. Thirty-seven sampling locations were sampled at depths of 0-2, 2-5, 5-8, and 8-11 inches, except where refusal was encountered for the analysis. The report of this work is attached to this ESD as *Attachment B.*

6. **The spatial distribution of manganese in residential soils is inconsistent with deposition of particulates from the smelter stacks.** See *Figure 1*. Manganese concentrations in soil adjacent to the former smelter are relatively low and below the residential cleanup standard for manganese specified in the ROD. Prevailing winds at the smelter are toward the northwest. However, the elevated manganese soil concentrations occur primarily to the southeast and to a lesser degree, to the east of the locations of the former smelter smokestacks. Moreover, the very highest levels of manganese are consistently clustered on a hillside slope on the other side of a ridge, facing away from the smelter entirely.

V.   Explanation of Significant Differences

The Comprehensive Environmental Response, Compensation, and Liability Act (CERCLA) defines background as naturally occurring substances in the environment that have not been influenced by human activity.[4]

CERCLA 104(a)(3)(A) provides that:

> "The President shall not provide for a removal or remedial action under this section in response to a release or threat of release—of a naturally occurring substance in its unaltered form, or altered solely through naturally occurring processes or phenomena, from a location where it is naturally found."

---

[4] For the purposes of cleanup, background can also include natural and human-made substances that are present in the environment as a result of human activities but are not specifically related to the CERCLA site in question.

This provision of the law is consistent with the fact that naturally occurring substances, being ubiquitous in the environment, cannot physically be "cleaned up". EPA finds that the localized levels of manganese in residential soils at the Site discussed in this ESD are naturally occurring and not related to the Site.

Accordingly, this ESD removes manganese (and its associated cleanup levels) as a COC under the ROD, and response actions in accordance with the ROD will not be taken to remediate it. It is noted that residential properties at which the exposure point concentration of manganese in soil were above the manganese cleanup level could still be remediated for other COCs such as arsenic and lead should the exposure point concentrations of those metals exceed their respective cleanup levels.

VI.   Support Agency Concurrence

ADEQ has concurred on this ESD for the Iron King Mine / Humboldt Smelter Superfund Site based on the letter dated December 20, 2024 (*Attachment C*).

VII.   Statutory Determinations

The modified remedy satisfies CERCLA § 121. EPA and ADEQ believe that the remedy remains protective of human health and the environment, complies with Federal and State requirements that are applicable or relevant and appropriate to this remedial action, and is cost effective.

VIII.   Public Participation Requirements

This document satisfies the public participation requirements under CERCLA Section 117(c) and the National Contingency Plan (NCP), 40 C.F.R. § 300.435(c)(2)(i). It will become part of the Administrative Record file for the Iron King Mine – Humboldt Smelter Superfund Site, as specified in the NCP, 40 C.F.R. § 300.825(a)(2). The Administrative Record file is available for public review on line at http://www.epa.gov/superfund/ironkingmine, at EPA Region IX, Superfund Records Center, 75 Hawthorne Street, San Francisco, CA 94105; and at the Dewey-Humboldt Public Library, 2735 Corral St., Humboldt, AZ 86329.

_____

Michael Montgomery, Director
Superfund and Emergency Response Division
EPA Region IX

ATTACHMENT A

26 Nov 2024

Neptune and Company, Inc.

1435 Garrison St.
Suite 201
Lakewood, Colorado 80215
720-746-1803
www.neptuneinc.org

TECHNICAL MEMORANDUM

From: Doug Anderson, John Carson

Through: Polona Carson, Contract Manager

To: Felicia Barnett, Work Assignment Manager
             Jeff Dhont, Remedial Project Manager, EPA Region 9
             Anne Lawrence, Remedial Project Manager, EPA Region 9
             Scott Grossman, EPA Environmental Response Team

Regarding: Analysis of Manganese Concentrations in Localized Areas Near the former
             Humboldt Smelter; Iron King Mine – Humboldt Smelter Superfund Site,
             Dewey-Humboldt, Arizona

This memorandum provides a synopsis of a multivariate compositional cluster analysis
performed by Neptune and Company (Neptune) to better understand the spatial and
compositional aspects of the surface soil concentrations of manganese near the former Humboldt
Smelter at the Iron King Mine – Humboldt Smelter Superfund Site. It is our opinion after
critically evaluating the compositional and spatial aspects of the sampling data for six metals that
the areas with substantially elevated manganese concentrations, especially east of the Agua Fria
River, are part of a mid-scale spatial pattern that indicate they are naturally occurring. These
areas have similar compositional patterns to the vast majority of the study area but have elevated
manganese due to higher iron concentrations.

Before discussing the compositional analysis, we consider whether there is a reasonable
possibility that manganese may have been emitted from the smelter stack as ash or fume particles
and been deposited in areas of high manganese concentration, especially in areas east of the
Agua Fria River. We believe that this is not the case. The volatility of manganese at the
temperatures of copper smelting (1500 °C, higher than those of lead smelting) is relatively low

and similar to that of iron at the same temperature. The equation is given in Brewer as $log(P/Pa) = 11.375 - 14100/(T/K)$, which translates to about 34 Pa at maximum expected copper smelting temperatures. This is about 3 ten-thousandths of one atmosphere, which is negligible and would result in virtually no stack emissions of manganese.

To gain a better understanding of manganese concentrations in the target areas, we explored the compositional signatures in the metals data in order to find common patterns. Arsenic, chromium, copper, lead, manganese, zinc, and iron were selected to represent the composition because they result in the largest possible complete data set, complete in the sense that each metal was measured in each sample.

The selected data are right-skewed in each variable. When looking at right-skewed variables, it is common to use a logarithmic transformation. In the case of compositions, the additive log ratio (ALR) transformation is often very useful. It is given by

$$ALR([As_i, Cr_i, Cu_i, Pb_i, Mn_i, Zn_i]; Fe_i) =$$
$$\left[log\left(\frac{As_i}{Fe_i}\right), log\left(\frac{Cr_i}{Fe_i}\right), log\left(\frac{Cu_i}{Fe_i}\right), log\left(\frac{Pb_i}{Fe_i}\right), log\left(\frac{Mn_i}{Fe_i}\right), log\left(\frac{Zn_i}{Fe_i}\right)\right].$$

where the subscript i indexes the samples. Seven original variables give 6 log ratios. An appropriate choice of denominator in the log ratios makes the compositional structure more visible than on the original scale.

In the process of exploring the compositional structure of the data, a powerful combination of tools brought to light some signature patterns in the data. The first tool is an algorithm for dimension reduction called Uniform Manifold Approximation & Projection (UMAP)[5]. This algorithm has been used in many practical fields with impressive results[6]. By applying the algorithm to the Additive Log Ratio (ALR) values, it calculates two new variables that help isolate the similarities and differences among the samples that are difficult to visualize in 6 dimensions.

Figure 1 shows the results of applying the UMAP algorithm to the ALR transformed data. The axes V1 and V2 are the axes of topological projection from the 6-dimensional manifold of the 2-dimensional manifold of the plot. To reduce the clutter on the plot due to the large number of sample results, hexagonal bins are used, and the shade of blue indicates the number of samples within each bin. There are two large groupings and a few small groupings which indicates there are two common signatures and potentially three anomalous signatures. The arrows on the plot give an approximate idea of how the original ALR variables load into the UMAP coordinates. This is somewhat analogous to the presentation of a biplot using principal component analysis (PCA). However, UMAP, combined with standard clustering techniques, makes those techniques

---

[5]   McInnes, L., Healy, J., & Melville, J. (2018). UMAP: Uniform manifold approximation and projection for dimension reduction. arXiv preprint arXiv:1802.03426.
[6]   Ghojogh, B., Ghodsi, A., Karray, F., & Crowley, M. (2021). Uniform manifold approximation and projection (UMAP) and its variants: tutorial and survey. arXiv preprint arXiv:2109.02508.

more effective[7]. The combination is much more effective for grouping than PCA, which was not designed to be and is not really a clustering technique.

Figure 3. Hexagonal bin scatter plot of the results of the UMAP algorithm applied to ALR transformed data.
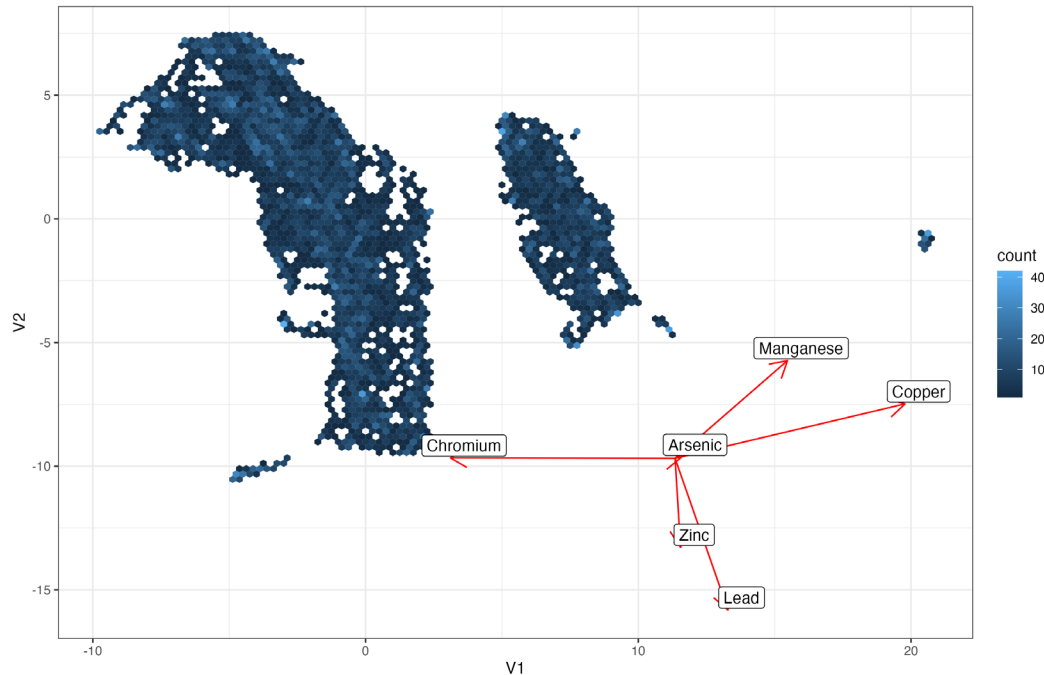
A second powerful technique called Density-Based Spatial Clustering of Applications with Noise (DBSCAN) focuses on the density of points to cluster points into groups. Applying DBSCAN to the dimension reduced space calculated by UMAP results in the clusters shown in Figure 2. Again, hexagonal binning is used to make the figure more interpretable.

---

7   Allaoui, M., Kherfi, M.L., Cheriet, A. (2020). Considerably Improving Clustering Algorithms Using UMAP Dimensionality Reduction Technique: A Comparative Study. In: El Moataz, A., Mammass, D., Mansouri, A., Nouboud, F. (eds) Image and Signal Processing. ICISP 2020. Lecture Notes in Computer Science(), vol 12119. Springer, Cham. https://doi.org/10.1007/978-3-030-51935-3_34

Figure 4. Hexagonal bin plot of cluster assignments calculated from DBSCAN algorithm.
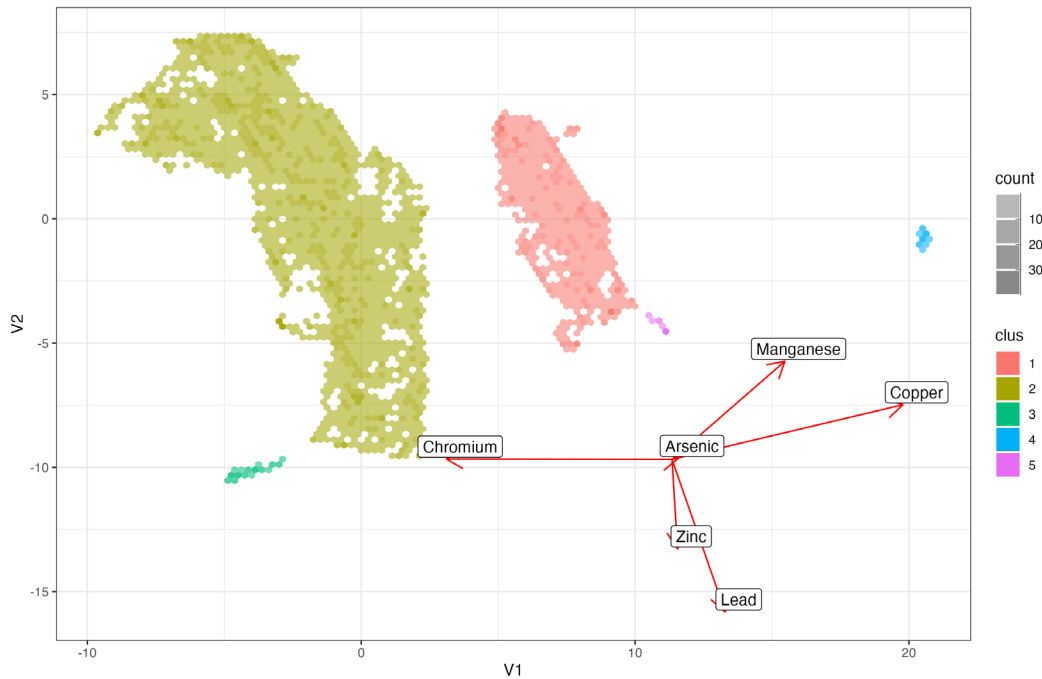

Figure 3 shows the spatial locations of samples for the five clusters. Sample results in compositional clusters 1 and 2 are common across the entire spatial domain. Sample results in compositional clusters 3, 4 and 5 show more unique spatial signatures, occurring only west of the Agua Fria River and relatively close to and around the Humboldt Smelter location. Although Neptune does not have descriptions of the materials at the locations of the cluster 3, 4 and 5 samples, upon closer review it appears that they correspond to various types of waste derived from site operations, and not from natural materials.

The results presented in Figure 3 are from the UMAP algorithm applied to the ALR transformed data with 15 nearest neighbors followed by DBSCAN clustering, computed with a maximum distance of 0.5 and a minimum cluster size of 5 samples. UMAP and DBSCAN were also used with variations of these parameters and gave similar results, including varying the number of nearest neighbors, using the distance matrix computed across the ALR transformed data, and using the distance matrix of the Aitchison compositional distance between samples.

An alternative dimension reduction technique called Multidimensional Scaling (MDS) was also implemented with the two aforementioned distance matrices. Multiple variations of MDS were implemented, including metric MDS and non-metric MDS using Sammon's transformation. Few differences were found between the results. The MDS algorithms were able to identify only one of the anomalous groups, cluster 4, with the remaining 4 signatures being combined into one signature.

Figure 5. Spatial plot of the hexagonal bins with color and panel indicating the cluster assignment from DBSCAN algorithm. The red path shows the Agua Fria River and the black circle shows the location of the Humboldt Smelter.
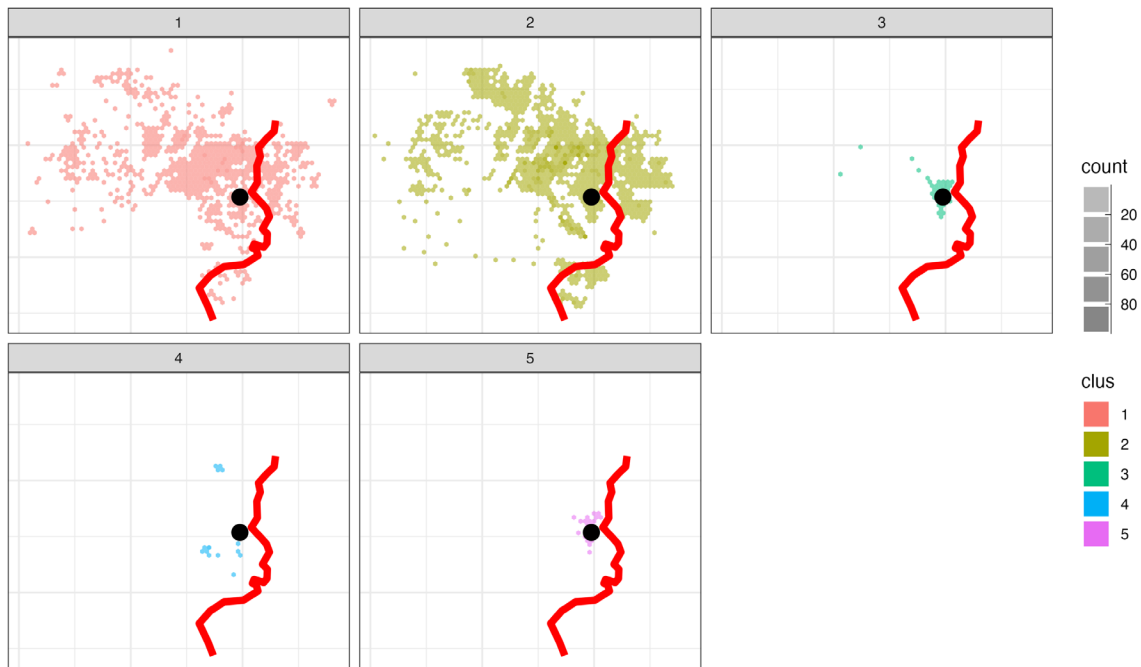

Table 1 gives the average ratio of metals to iron (mean of exponentiated ALR values) by cluster. In examining Table 1, Cluster 4 stands out as having the highest average ratio to iron for all the metals. Cluster 2 on average has the lowest ratio to iron for all the metals except for chromium where Cluster 1 has a lower ratio on average. Cluster 1 has the next lowest ratios to iron, on average, for the other metals. Clusters 3 has a higher ratio to iron on average than Cluster 5 for arsenic, lead, manganese, and zinc, while Cluster 5 has a higher ratio to iron on average for chromium and copper compared to Cluster 3.

Table 1. Cluster group counts and average ratios to iron for 6 metals

Cluster	Count	As/Fe	Cr/Fe	Cu/Fe	Pb/Fe	Mn/Fe	Zn/Fe
1	2947	0.0027	0.0077	0.0009	0.0059	0.0301	0.0141
2	10,425	0.0020	0.0011	0.0021	0.0040	0.0212	0.0079
3	205	0.0064	0.0160	0.0201	0.0618	0.0570	0.314
4	100	3.98	0.898	3.23	6.47	603	11.00
5	61	0.0041	0.389	0.0296	0.0480	0.0471	0.235

Figure 4 displays the ALR data by element and cluster using boxplots. A box plot, also known as a box-and-whisker plot, is a standardized way of displaying the distribution of a data set based on its five-number summary: minimum, first quartile (Q1), median, third quartile (Q3), and maximum. It consists of a box with a line inside, and extended lines (whiskers) attached to each side. The box represents the interquartile range (IQR), and the line inside the box marks the median. Outliers, if any, are plotted as individual points beyond the whiskers. Box plots are

useful for identifying the distribution's skewness, outliers, and overall variability. They can display one or more groups of numerical data, making it easy to compare the distributions side-by-side.

The ALR values are in log scale compared to the values in Table 1. Clusters 1 and 2 appear to be the most similar to each other of any of the clusters.

Figure 6. Boxplots of ALR by element and cluster
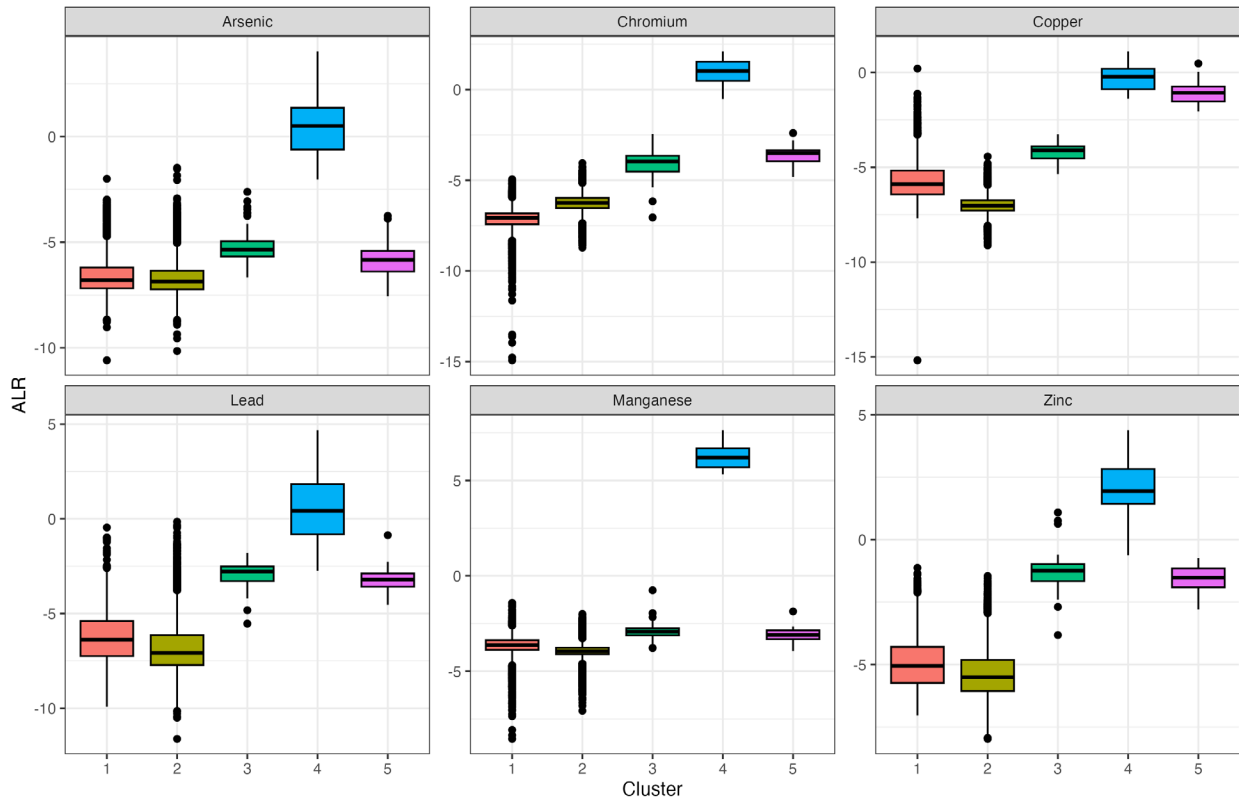
Table 2 gives the average concentration by cluster. Cluster 5 has the largest concentrations on average for chromium, copper, lead, and zinc, but relatively low average concentrations in arsenic, iron, and manganese. Cluster 4 has extremely low concentrations on average for iron, the highest average concentration for arsenic and extremely high manganese concentrations compared to the other clusters. Cluster 3 has relatively high concentrations of lead and zinc on average compared to the other clusters. Samples on average in Cluster 2 have the highest iron content, but relatively low chromium, copper, lead, and zinc. Lastly, Cluster 1 has relatively high concentrations of arsenic, copper, and iron, on average, but typically low chromium, lead, and zinc. Again, only clusters 1 and 2 appear to represent samples collected from natural materials, while Figure 3 shows that clusters 3, 4 and 5 occur in areas where waste materials are expected.

Table 2. Cluster group counts and average concentrations (mg/kg) for 7 metals

Cluster	Count	As	Cr	Cu	Fe	Pb	Mn	Zn
1	2947	154	28	235	31,960	240	868	589
2	10,425	94	75	39	40,564	201	887	305
3	205	69	169	143	11,057	592	547	2989
4	100	209	176	50	69	352	32,246	631
5	61	73	529	6790	18,750	885	798	3960

Figure 5 displays the log concentration data by element and cluster using boxplots. Again, clusters 1 and 2 appear to be the most similar to each other of any of the clusters.

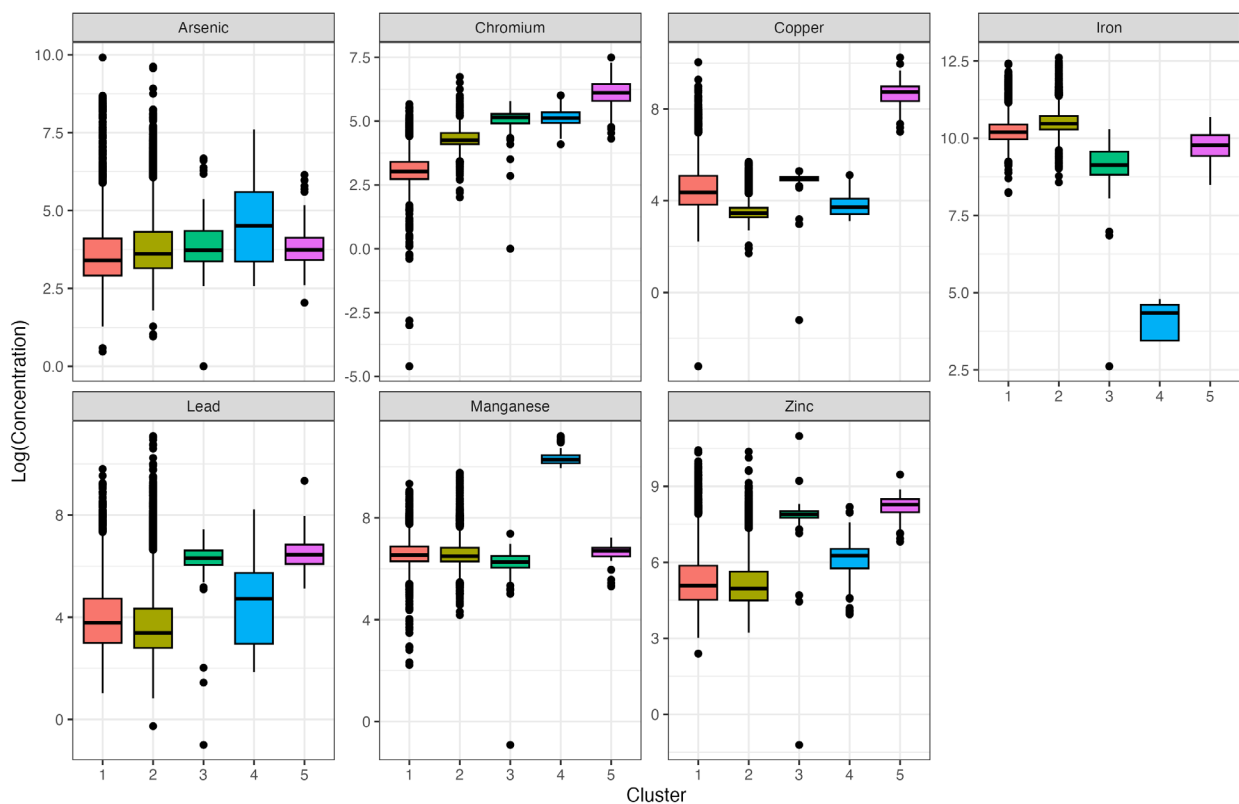*Figure 7. Boxplots of log concentration by element and cluster*

Summaries of the clusters are presented in the Tables section that follows the References. Table 3 presents measures of center and spread (median, min, max, mean and standard deviation) for each metal within each cluster in the ALR scale. Table 4 presents the same measures in the original concentration scale. Table 5 and Table 6 present the correlation and covariance structures in the ALR scale for each cluster. Table 7 and Table 8 present the correlation and covariance structures in the original concentration scale for each cluster.

Figure 6 shows hexagonal binned scatterplots comparing the log concentrations of manganese to the log concentrations of iron. The color and panel indicate the cluster assignments of each sample. The linear trend in cluster 4 is most anomalous with its low iron content (in many cases

nondetect) and flat slope. The linear trend in cluster 1 has a slope intermediate between that of cluster 4 and the other clusters. The other three clusters have relatively similar relationships between manganese and iron. Except for cluster 4, the manganese-iron relationship is not a strong compositional differentiator between the clusters.

Figure 8. Log(Manganese) vs. Log(Iron) by cluster. Regression lines are plotted over the hexagonal bins.
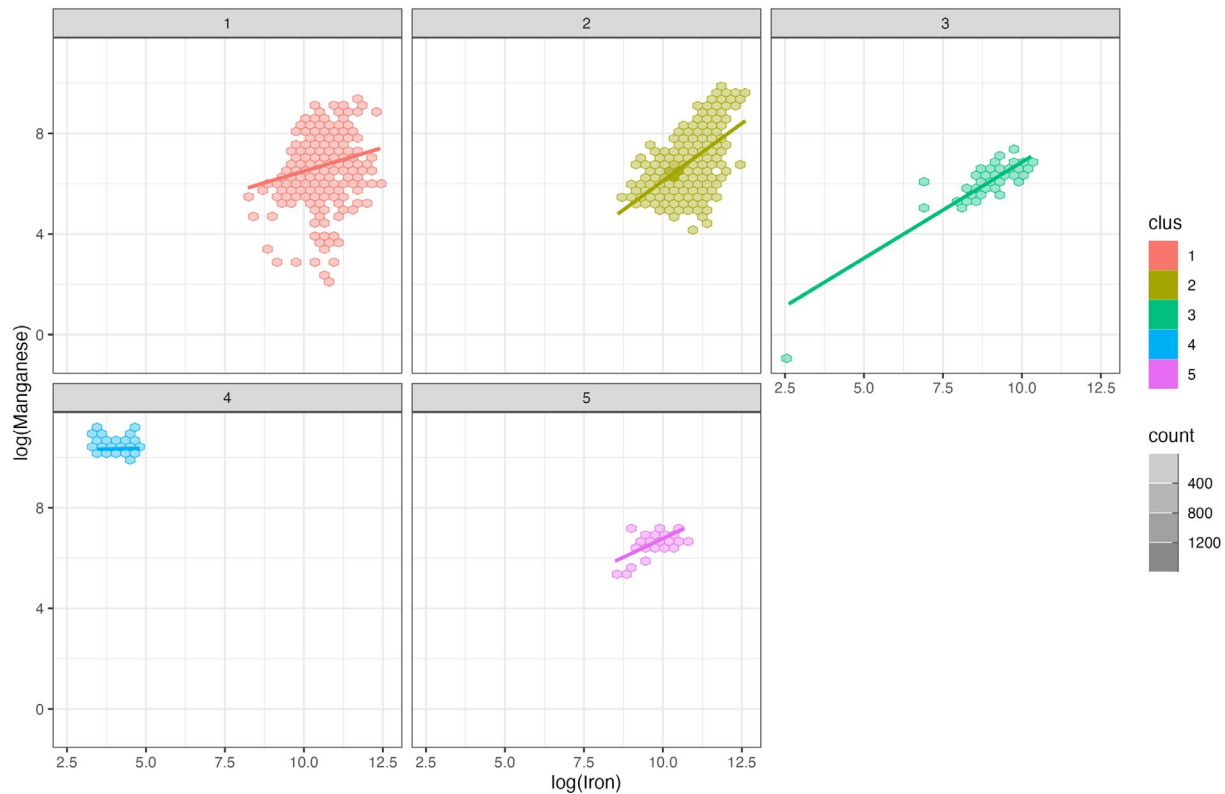
Conclusions

The compositions associated with clusters 1 and 2 are widespread across the site and are found in abundance in every direction from the location of the former smelter. If manganese was relatively enriched in the fumes or ash from the smelter and was deposited downwind of the smelter, and specifically east of the Agua Fria River, then there should be a detectable compositional signature of this deposition. But there is no indication of this at all. The two compositions represented in the main clusters are consistently found across the site. These clusters both feature increasing manganese concentration with increasing iron concentration, which has an increasing spatial trend from west to east across the eastern portion of the overall site.

The anomalous groups, clusters 3-5, are only found west of the Agua Fria and in areas relatively near the former smelter operations. These seem likely to be impacted in some way by site operations, but in what way is not clear at this point.

Given the low volatility of manganese combined with the results from this analysis, there is no evidence to indicate levels of manganese east of the Agua Fria River are the product of site operations. All samples east of the river follow similar compositional patterns to those found across the entire spatial domain.

References

Brewer (1946). The thermodynamic and physical properties of the elements, Report for the Manhattan Project.

Hahsler M, Piekenbrock M, Doran D (2019). "dbscan: Fast Density-Based Clustering with R." *Journal of Statistical Software*, **91**(1), 1–30. doi:10.18637/jss.v091.i01.

Konopka T (2023). "umap: Uniform Manifold Approximation and Projection." R package version 0.2.10.0, https://CRAN.R-project.org/package=umap.

McInnes, L., Healy, J., & Melville, J. (2020). "UMAP: Uniform Manifold Approximation and Projection for Dimension Reduction." *arXiv [Stat.ML]*. Retrieved from http://arxiv.org/abs/1802.03426

Van den Boogaart KG, Tolosana-Delgado R, Bren M (2024). "compositions: Compositional Data Analysis." R package version 2.0-8, https://CRAN.R-project.org/package=compositions.

Tables

Table 3. Summary statistics of each metal within a cluster. The summaries were calculated on the ALR scale.

Cluster	Metal	Median [Min., Max.]	Mean (SD)
1	Arsenic	-6.8 [-10.6, -2]	-6.57 (0.95)
	Chromium	-7.07 [-14.93, -4.94]	-7.15 (0.71)
	Copper	-5.89 [-15.18, 0.2]	-5.67 (1.03)
	Lead	-6.38 [-9.92, -0.46]	-6.24 (1.34)
	Manganese	-3.63 [-8.55, -1.42]	-3.66 (0.62)
	Zinc	-5.06 [-7.04, -1.13]	-4.92 (1.05)
2	Arsenic	-6.86 [-10.15, -1.48]	-6.69 (0.82)
	Chromium	-6.25 [-8.71, -4.05]	-6.27 (0.46)
	Copper	-7.03 [-9.12, -4.43]	-6.98 (0.48)
	Lead	-7.08 [-11.61, -0.16]	-6.83 (1.31)
	Manganese	-3.95 [-7.08, -2]	-3.94 (0.41)
	Zinc	-5.51 [-7.98, -1.46]	-5.39 (0.95)
3	Arsenic	-5.35 [-6.67, -2.62]	-5.29 (0.61)
	Chromium	-3.96 [-7.05, -2.44]	-4.09 (0.64)
	Copper	-4.11 [-5.35, -3.26]	-4.23 (0.46)
	Lead	-2.79 [-5.53, -1.81]	-2.91 (0.55)
	Manganese	-2.92 [-3.78, -0.76]	-2.94 (0.35)
	Zinc	-1.25 [-3.82, 1.09]	-1.33 (0.55)
4	Arsenic	0.51 [-2.03, 4.03]	0.46 (1.37)
	Chromium	1.03 [-0.51, 2.1]	1.01 (0.6)
	Copper	-0.23 [-1.39, 1.1]	-0.31 (0.65)
	Lead	0.41 [-2.75, 4.68]	0.49 (1.68)
	Manganese	6.2 [5.33, 7.64]	6.23 (0.58)
	Zinc	1.94 [-0.62, 4.39]	1.96 (1.01)
5	Arsenic	-5.84 [-7.56, -3.75]	-5.84 (0.8)
	Chromium	-3.5 [-4.81, -2.39]	-3.64 (0.52)
	Copper	-1.08 [-2.06, 0.47]	-1.09 (0.53)
	Lead	-3.2 [-4.54, -0.86]	-3.27 (0.62)
	Manganese	-3.1 [-3.94, -1.87]	-3.11 (0.34)
	Zinc	-1.52 [-2.79, -0.74]	-1.56 (0.49)

Table 4. Correlation matrices for each cluster calculated on the ALR scale.

Cluster		As	Cr	Cu	Pb	Mn	Zn
1	As	1.00	-0.39	0.35	0.74	-0.43	0.71
	Cr	-0.39	1.00	0.22	-0.17	0.56	-0.17
	Cu	0.35	0.22	1.00	0.59	0.04	0.59
	Pb	0.74	-0.17	0.59	1.00	-0.25	0.89
	Mn	-0.43	0.56	0.04	-0.25	1.00	-0.17
	Zn	0.71	-0.17	0.59	0.89	-0.17	1.00
2	As	1.00	-0.02	0.29	0.70	-0.37	0.59
	Cr	-0.02	1.00	0.60	0.22	0.13	0.26
	Cu	0.29	0.60	1.00	0.62	0.00	0.69
	Pb	0.70	0.22	0.62	1.00	-0.28	0.83
	Mn	-0.37	0.13	0.00	-0.28	1.00	-0.21
	Zn	0.59	0.26	0.69	0.83	-0.21	1.00
3	As	1.00	0.04	0.04	0.13	-0.11	-0.12
	Cr	0.04	1.00	0.85	0.39	0.55	0.42
	Cu	0.04	0.85	1.00	0.56	0.70	0.73
	Pb	0.13	0.39	0.56	1.00	0.13	0.68
	Mn	-0.11	0.55	0.70	0.13	1.00	0.55
	Zn	-0.12	0.42	0.73	0.68	0.55	1.00
4	As	1.00	0.19	0.46	0.90	0.60	0.58
	Cr	0.19	1.00	0.72	0.23	0.74	0.43
	Cu	0.46	0.72	1.00	0.42	0.71	0.67
	Pb	0.90	0.23	0.42	1.00	0.52	0.65
	Mn	0.60	0.74	0.71	0.52	1.00	0.54
	Zn	0.58	0.43	0.67	0.65	0.54	1.00
5	As	1.00	0.05	0.15	0.29	0.06	0.26
	Cr	0.05	1.00	0.53	0.43	0.66	0.59
	Cu	0.15	0.53	1.00	0.50	0.59	0.72
	Pb	0.29	0.43	0.50	1.00	0.44	0.65
	Mn	0.06	0.66	0.59	0.44	1.00	0.72
	Zn	0.26	0.59	0.72	0.65	0.72	1.00

Table 5. Covariance matrices for each cluster calculated on the ALR scale.

Cluster		As	Cr	Cu	Pb	Mn	Zn
1	As	0.91	-0.26	0.35	0.95	-0.25	0.71
	Cr	-0.26	0.50	0.16	-0.16	0.24	-0.12
	Cu	0.35	0.16	1.06	0.81	0.02	0.64
	Pb	0.95	-0.16	0.81	1.79	-0.20	1.25
	Mn	-0.25	0.24	0.02	-0.20	0.38	-0.11
	Zn	0.71	-0.12	0.64	1.25	-0.11	1.09
2	As	0.66	-0.01	0.11	0.75	-0.12	0.46
	Cr	-0.01	0.21	0.13	0.13	0.02	0.11
	Cu	0.11	0.13	0.23	0.39	0.00	0.32
	Pb	0.75	0.13	0.39	1.72	-0.15	1.04
	Mn	-0.12	0.02	0.00	-0.15	0.17	-0.08
	Zn	0.46	0.11	0.32	1.04	-0.08	0.91
3	As	0.38	0.01	0.01	0.04	-0.02	-0.04
	Cr	0.01	0.41	0.25	0.14	0.13	0.15
	Cu	0.01	0.25	0.21	0.14	0.11	0.18
	Pb	0.04	0.14	0.14	0.30	0.03	0.20
	Mn	-0.02	0.13	0.11	0.03	0.13	0.11
	Zn	-0.04	0.15	0.18	0.20	0.11	0.30
4	As	1.87	0.16	0.41	2.08	0.48	0.81
	Cr	0.16	0.36	0.28	0.23	0.26	0.26
	Cu	0.41	0.28	0.42	0.46	0.27	0.44
	Pb	2.08	0.23	0.46	2.82	0.50	1.10
	Mn	0.48	0.26	0.27	0.50	0.33	0.31
	Zn	0.81	0.26	0.44	1.10	0.31	1.03
5	As	0.64	0.02	0.06	0.14	0.02	0.10
	Cr	0.02	0.27	0.14	0.14	0.12	0.15
	Cu	0.06	0.14	0.28	0.16	0.11	0.19
	Pb	0.14	0.14	0.16	0.39	0.09	0.20
	Mn	0.02	0.12	0.11	0.09	0.11	0.12
	Zn	0.10	0.15	0.19	0.20	0.12	0.24

Table 6. Summary statistics of each metal within a cluster. The summaries were calculated on the original concentration scale.

Cluster	Metal	Median [Min., Max.]	Mean (SD)
1	Arsenic	30 [1.6, 20200]	154.25 (667.29)
	Chromium	20.5 [0.01, 288]	28.12 (25.7)
	Copper	78.5 [0.04, 22900]	234.56 (716.02)
	Iron	26700 [3740, 247000]	31959.89 (20421.3)
	Lead	43.9 [2.8, 18100]	240.02 (867.95)
	Manganese	691 [9.2, 11400]	868.39 (720.44)
	Zinc	161 [11, 33700]	589.09 (1906.38)
2	Arsenic	37 [2.6, 15100]	94.32 (304.59)
	Chromium	70.4 [7.5, 841]	74.71 (26.53)
	Copper	31.6 [5.5, 299]	38.64 (23.38)
	Iron	35200 [5270, 3e+05]	40564.26 (19522.7)
	Lead	29.6 [0.77, 65700]	200.7 (1555.87)
	Manganese	660 [65.3, 17500]	887.1 (964.89)
	Zinc	143 [25.3, 31800]	304.6 (682.57)
3	Arsenic	41.6 [1, 792]	68.67 (97.66)
	Chromium	172 [1, 324]	169.09 (47.49)
	Copper	146 [0.3, 199]	143.15 (23.44)
	Iron	9250 [13.7, 29500]	11056.67 (5760.28)
	Lead	554 [0.37, 1720]	591.75 (254.31)
	Manganese	526 [0.4, 1600]	547.32 (196.34)
	Zinc	2670 [0.3, 58900]	2988.71 (4036.14)
4	Arsenic	91.05 [13.1, 2000]	209.44 (310.16)
	Chromium	167 [59.9, 406]	175.98 (59.49)
	Copper	41.5 [22.4, 167]	50.28 (27.96)
	Iron	77.2 [31.5, 121]	69.08 (31.88)
	Lead	113 [6.42, 3720]	352.44 (715.06)
	Manganese	29200 [21100, 74000]	32246 (10145.53)
	Zinc	526 [51.6, 3600]	630.92 (644.09)
5	Arsenic	42.2 [7.7, 467]	72.89 (91.08)
	Chromium	451 [74.8, 1790]	528.83 (330.81)
	Copper	6240 [1100, 28100]	6790.49 (4521.3)
	Iron	17500 [4840, 43500]	18749.67 (8546.72)
	Lead	635 [169, 11400]	884.64 (1429.62)
	Manganese	819 [202, 1380]	798.07 (242.75)
	Zinc	3940 [911, 12900]	3959.85 (1864.98)

Table 7. Correlation matrices for each cluster calculated on the original concentration scale.

Cluster		As	Cr	Cu	Fe	Pb	Mn	Zn
1	As	1.00	-0.05	0.08	0.65	0.56	-0.02	0.60
	Cr	-0.05	1.00	0.14	0.23	-0.06	0.23	-0.06
	Cu	0.08	0.14	1.00	0.12	0.16	0.03	0.22
	Fe	0.65	0.23	0.12	1.00	0.47	0.28	0.63
	Pb	0.56	-0.06	0.16	0.47	1.00	-0.04	0.60
	Mn	-0.02	0.23	0.03	0.28	-0.04	1.00	0.05
	Zn	0.60	-0.06	0.22	0.63	0.60	0.05	1.00
2	As	1.00	0.07	0.24	0.25	0.68	-0.01	0.40
	Cr	0.07	1.00	0.32	0.09	0.04	0.07	0.14
	Cu	0.24	0.32	1.00	0.16	0.21	0.03	0.50
	Fe	0.25	0.09	0.16	1.00	0.15	0.72	0.15
	Pb	0.68	0.04	0.21	0.15	1.00	-0.02	0.57
	Mn	-0.01	0.07	0.03	0.72	-0.02	1.00	0.00
	Zn	0.40	0.14	0.50	0.15	0.57	0.00	1.00
3	As	1.00	-0.26	0.07	0.45	0.50	0.19	0.00
	Cr	-0.26	1.00	0.38	-0.09	0.01	0.00	-0.21
	Cu	0.07	0.38	1.00	0.33	0.31	0.56	0.15
	Fe	0.45	-0.09	0.33	1.00	0.39	0.72	0.14
	Pb	0.50	0.01	0.31	0.39	1.00	0.21	0.18
	Mn	0.19	0.00	0.56	0.72	0.21	1.00	0.43
	Zn	0.00	-0.21	0.15	0.14	0.18	0.43	1.00
4	As	1.00	-0.27	0.10	-0.01	0.80	0.80	0.50
	Cr	-0.27	1.00	0.52	0.07	-0.14	-0.04	0.22
	Cu	0.10	0.52	1.00	0.12	0.08	0.26	0.47
	Fe	-0.01	0.07	0.12	1.00	0.02	0.02	0.11
	Pb	0.80	-0.14	0.08	0.02	1.00	0.60	0.64
	Mn	0.80	-0.04	0.26	0.02	0.60	1.00	0.44
	Zn	0.50	0.22	0.47	0.11	0.64	0.44	1.00
5	As	1.00	0.13	0.10	0.24	0.15	0.06	0.08
	Cr	0.13	1.00	0.31	0.48	0.20	0.60	0.40
	Cu	0.10	0.31	1.00	0.30	0.48	0.41	0.59
	Fe	0.24	0.48	0.30	1.00	0.22	0.62	0.26
	Pb	0.15	0.20	0.48	0.22	1.00	0.25	0.70
	Mn	0.06	0.60	0.41	0.62	0.25	1.00	0.54
	Zn	0.08	0.40	0.59	0.26	0.70	0.54	1.00

Table 8. Covariance matrices for each cluster calculated on the original concentration scale.

Cluster			As	Cr	Cu	Fe	Pb	Mn	Zn
1		As	4.45E+05	-9.35E+02	3.93E+04	8.80E+06	3.27E+05	-9.02E+03	7.63E+05
		Cr	-9.35E+02	6.61E+02	2.51E+03	1.19E+05	-1.40E+03	4.26E+03	-2.98E+03
		Cu	3.93E+04	2.51E+03	5.13E+05	1.74E+06	9.93E+04	1.57E+04	2.95E+05
		Fe	8.80E+06	1.19E+05	1.74E+06	4.17E+08	8.30E+06	4.16E+06	2.46E+07
		Pb	3.27E+05	-1.40E+03	9.93E+04	8.30E+06	7.53E+05	-2.32E+04	9.87E+05
		Mn	-9.02E+03	4.26E+03	1.57E+04	4.16E+06	-2.32E+04	5.19E+05	6.71E+04
		Zn	7.63E+05	-2.98E+03	2.95E+05	2.46E+07	9.87E+05	6.71E+04	3.63E+06
2		As	9.28E+04	5.41E+02	1.74E+03	1.47E+06	3.22E+05	-2.61E+03	8.37E+04
		Cr	5.41E+02	7.04E+02	1.98E+02	4.58E+04	1.83E+03	1.83E+03	2.46E+03
		Cu	1.74E+03	1.98E+02	5.46E+02	7.28E+04	7.48E+03	6.48E+02	8.01E+03
		Fe	1.47E+06	4.58E+04	7.28E+04	3.81E+08	4.64E+06	1.35E+07	2.02E+06
		Pb	3.22E+05	1.83E+03	7.48E+03	4.64E+06	2.42E+06	-2.38E+04	6.02E+05
		Mn	-2.61E+03	1.83E+03	6.48E+02	1.35E+07	-2.38E+04	9.31E+05	-2.50E+03
		Zn	8.37E+04	2.46E+03	8.01E+03	2.02E+06	6.02E+05	-2.50E+03	4.66E+05
3		As	9.54E+03	-1.22E+03	1.51E+02	2.53E+05	1.25E+04	3.73E+03	-7.27E+02
		Cr	-1.22E+03	2.25E+03	4.25E+02	-2.51E+04	1.24E+02	-4.65E+01	-4.07E+04
		Cu	1.51E+02	4.25E+02	5.49E+02	4.41E+04	1.83E+03	2.56E+03	1.42E+04
		Fe	2.53E+05	-2.51E+04	4.41E+04	3.32E+07	5.69E+05	8.13E+05	3.27E+06
		Pb	1.25E+04	1.24E+02	1.83E+03	5.69E+05	6.47E+04	1.03E+04	1.83E+05
		Mn	3.73E+03	-4.65E+01	2.56E+03	8.13E+05	1.03E+04	3.85E+04	3.43E+05
		Zn	-7.27E+02	-4.07E+04	1.42E+04	3.27E+06	1.83E+05	3.43E+05	1.63E+07
4		As	9.62E+04	-4.99E+03	9.02E+02	-1.13E+02	1.78E+05	2.53E+06	9.93E+04
		Cr	-4.99E+03	3.54E+03	8.68E+02	1.39E+02	-5.85E+03	-2.71E+04	8.54E+03
		Cu	9.02E+02	8.68E+02	7.82E+02	1.09E+02	1.59E+03	7.49E+04	8.46E+03
		Fe	-1.13E+02	1.39E+02	1.09E+02	1.02E+03	4.13E+02	6.46E+03	2.35E+03
		Pb	1.78E+05	-5.85E+03	1.59E+03	4.13E+02	5.11E+05	4.37E+06	2.94E+05
		Mn	2.53E+06	-2.71E+04	7.49E+04	6.46E+03	4.37E+06	1.03E+08	2.86E+06
		Zn	9.93E+04	8.54E+03	8.46E+03	2.35E+03	2.94E+05	2.86E+06	4.15E+05
5		As	8.30E+03	3.97E+03	4.22E+04	1.90E+05	1.97E+04	1.26E+03	1.33E+04
		Cr	3.97E+03	1.09E+05	4.62E+05	1.36E+06	9.62E+04	4.81E+04	2.49E+05
		Cu	4.22E+04	4.62E+05	2.04E+07	1.14E+07	3.07E+06	4.48E+05	5.01E+06
		Fe	1.90E+05	1.36E+06	1.14E+07	7.30E+07	2.65E+06	1.28E+06	4.12E+06
		Pb	1.97E+04	9.62E+04	3.07E+06	2.65E+06	2.04E+06	8.81E+04	1.88E+06
		Mn	1.26E+03	4.81E+04	4.48E+05	1.28E+06	8.81E+04	5.89E+04	2.45E+05
		Zn	1.33E+04	2.49E+05	5.01E+06	4.12E+06	1.88E+06	2.45E+05	3.48E+06

ATTACHMENT B

Neptune and Company, Inc.

1435 Garrison St.
Suite 201
Lakewood, Colorado 80215
720-746-1803
www.neptuneinc.org

13 Nov 2024

TECHNICAL MEMORANDUM

From: Doug Anderson, John Carson
             Neptune and Company, Inc.

Through: Polona Carson, Contract Manager

To: Felicia Barnett, Work Assignment Manager
             Jeff Dhont, Remedial Project Manager, EPA Region 9
             Anne Lawrence, Remedial Project Manager, EPA Region 9
             Scott Grossman, EPA Environmental Response Team

Regarding: Analysis of Manganese Concentrations at Various Depths in Background
             Areas Near the former Humboldt Smelter; Iron King Mine – Humboldt
             Smelter Superfund Site, Dewey-Humboldt, Arizona

This memorandum provides a synopsis of a spatial and compositional analysis performed by Neptune and Company (Neptune) to better understand the spatial and compositional aspects of the surface soil concentrations of manganese near the former Humboldt Smelter at the Iron King Mine – Humboldt Smelter Superfund Site. A special background study was conducted in which samples were collected at 37 undisturbed locations east of the Agua Fria River with cores taken at multiple depths. The objective was to determine whether manganese concentrations were higher at surface than at depth. The study found that manganese concentrations were not higher at surface than at depth. It is our opinion after critically evaluating the compositional and spatial aspects of the sampling data there is no impact to manganese concentrations from smelter emissions.

Figure 1 below shows the sampling locations. The site of the former smelter is shown as a black dot. The location of the Agua Fria River is shown as a red path. The sampling locations are shown as crosses. Some of them are relatively near the former smelter; others are more distant. As part of the analysis, distance to the former smelter location was computed for each sampling location. The sampling intervals at each location started at depths of 0, 2, 5, and 8 inches, unless refusal was encountered.

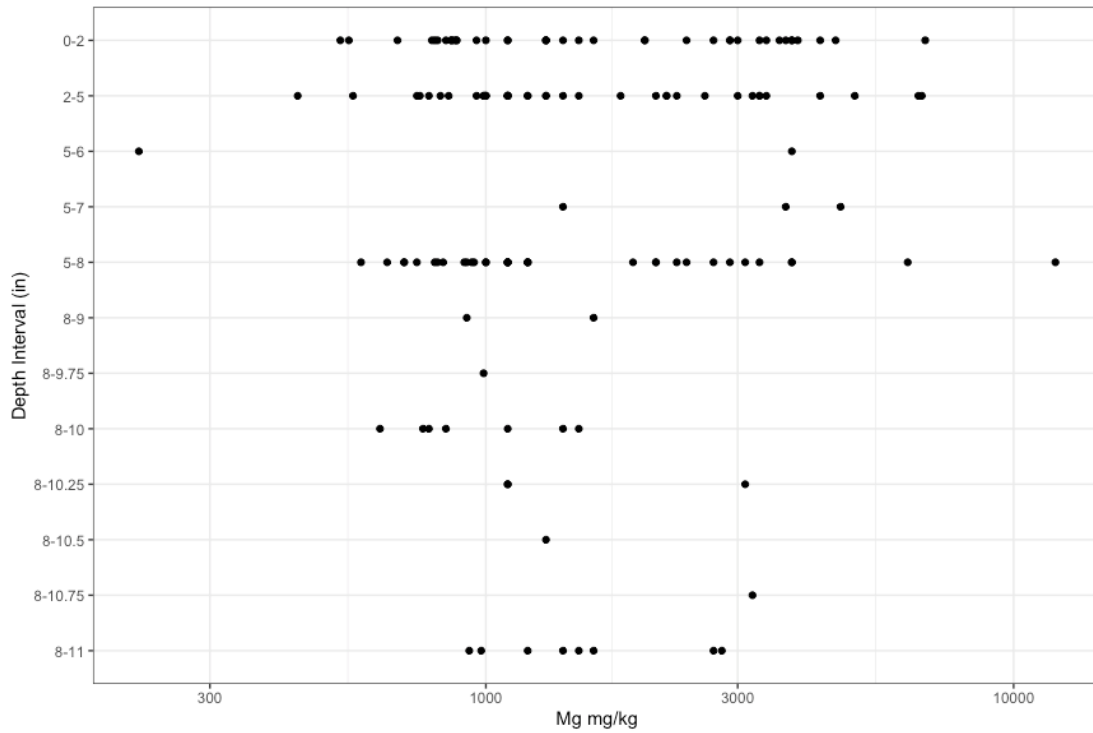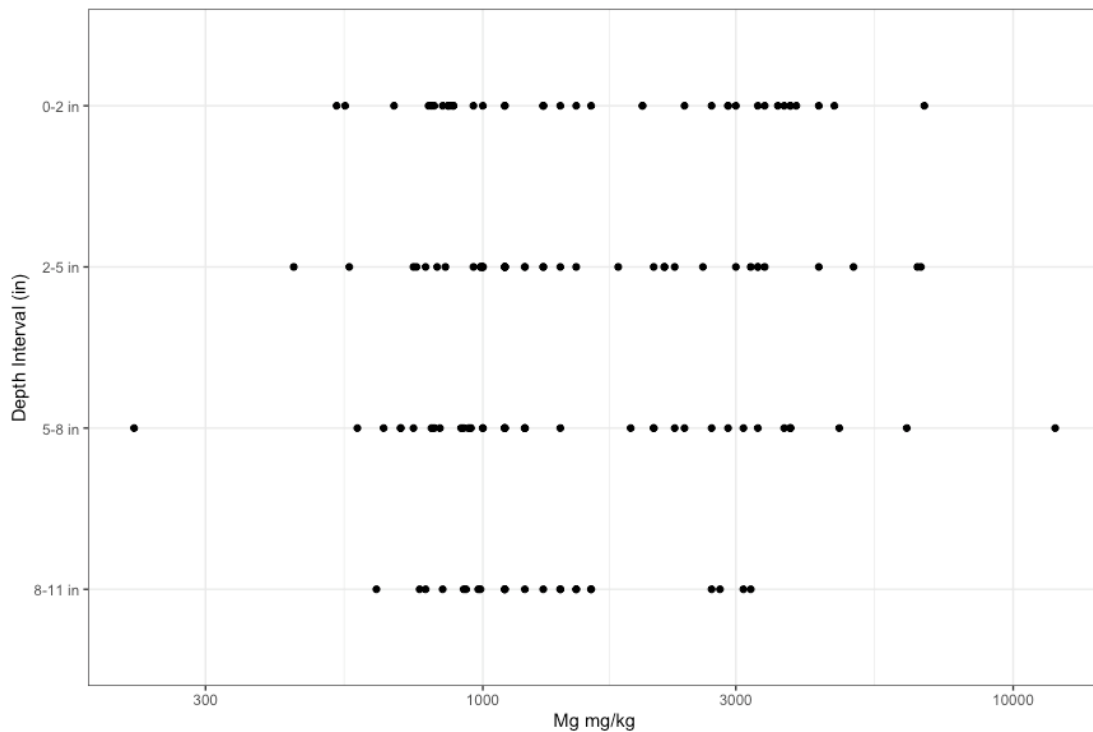*Figure 9. Mg concencentrations (mg/kg) at each unique depth interval.*

Figure 10. Mg concentrations (mg/kg) at depth intervals of 0-2 in, 2-5 in, 5-8 in, and 8-11 in. Samples were assigned the depth interval for which there was overlap.

Initially, t-tests were performed to compare surface manganese concentrations to subsurface. Using the grouping, surface versus subsurface, the Fligner-Killeen test, a robust test of equality of variances, failed to reject equality of variances for the two groups (p-value = 0.10). Accordingly, a two-sample t-test with equal variances was used to compare mean manganese concentrations at surface and subsurface. It found no indication of differing means (p-value = 0.56). A paired t-test, by location, using averages of the subsurface samples, also found no indication of differing means (p-value = 0.91).

Figure 11. Sampling locations for special background study.
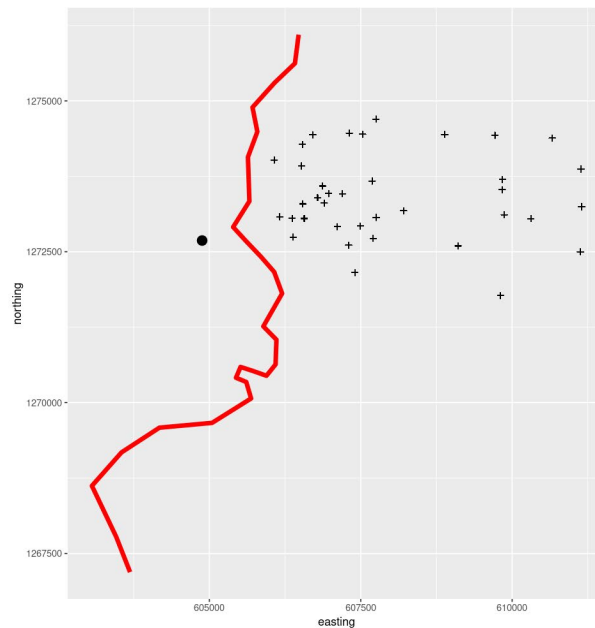
In order to determine whether there were more subtle differences in manganese concentration with depth, and also to consider distance from the former smelter location, a mixed effects regression was used, with location being a random effect. The data are plotted in Figure 2 below. No obvious trends are apparent.

Figure 12. Mn concentrations versus interval mid-point depth by location.
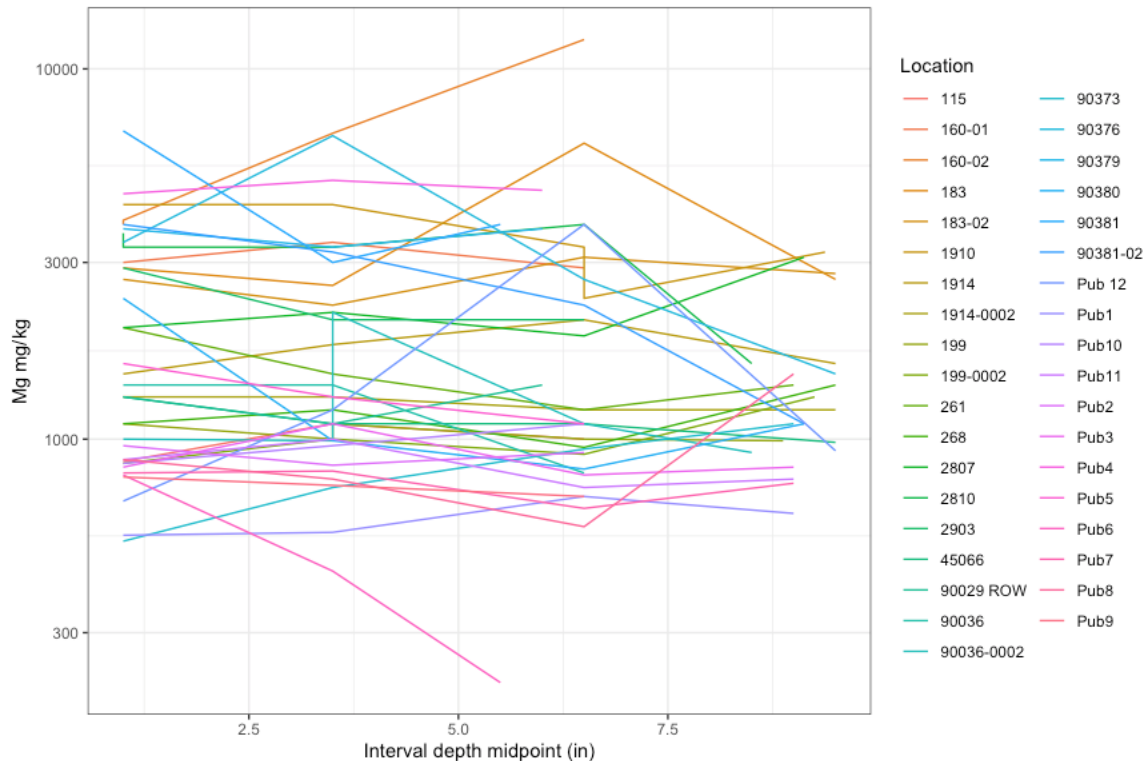
The best fitting model included a term decreasing in distance from the former smelter location and a random effect for sampling location. Depth of the sample core was not found to be a significant predictor of concentration. This indicated no change of concentration with depth but a decreasing trend with increasing distance from the former smelter location.

Next, we considered the log-ratio of manganese to iron, since this was very important in the compositional analysis. The best fitting model included a term decreasing in distance from the former smelter location, a term decreasing in depth of the core, and a random effect for sampling location. Since, the manganese to iron ratio was decreasing with depth of the core, we modeled iron concentrations. The best fitting model included a term decreasing in the Northing coordinate of the sampling location (at least within the footprint of the study design), a term increasing in depth of the core, and a random effect for sampling location. It makes sense that iron concentrations are increasing with depth given that manganese concentrations are constant with depth but the log-ratio of manganese to iron is decreasing with depth.
The analysis was performed in R.

Conclusion
Significant manganese contamination above background levels caused by either smelter stack emissions or wind blown dust from waste materials would be evidenced by a signature of increasing manganese concentrations at the surface. This study was designed to find such a signature if it existed. In fact, it has found no evidence to support contamination due to site operations.

ATTACHMENT C
State of Arizona Concurrence Letter
(See next page)

Arizona Department of Environmental Quality

Katie Hobbs
Governor

Karen Peters
Deputy Director

Via email

December 20, 2024

FPU 25-116

Mr. Jeffrey A. Dhont
U.S. Environmental Protection Agency, Region IX
75 Hawthorne Street Mail Stop SFD-6-2
San Francisco, CA 94105

Re: ADEQ Review of the *Draft Explanation of Significant Differences to the October 30, 2023 Record of Decision for the Iron King Mine – Humboldt Smelter Superfund Site* for the Iron King Mine – Humboldt Smelter Superfund Site, Dewey-Humboldt, Arizona received December 19, 2024

Dear Mr. Dhont:

The Arizona Department of Environmental Quality (ADEQ) Federal Projects Unit (FPU) has completed the review of the above referenced draft Explanation of Significant Differences (ESD) to the October 30, 2023 Record of Decision (ROD). ADEQ concurs with the draft ESD and looks forward to working with EPA in implementing the remedy.

If you have any questions, please contact me at 602-771-0167 or

kane-devries.katelyn@azdeq.gov.

Phoenix Office
1110 W. Washington St. | Phoenix, AZ 85007
602-771-2300

Southern Regional Office
400 W. Congress St. | Suite 433 | Tucson, AZ 85701
520-628-6733

azdeq.gov

Page 2 of 2

Regards,

Katelyn Kane-DeVries, RG
Project Manager/Hydrogeologist

C: Mekaela Bennett, Tetra Tech